Articles

Diverse Solid-State and Solution Structures within a Series of Hexaamine Dicopper(II) Complexes

Paul V. Bernhardt

Department of Chemistry, University of Queensland, Brisbane 4072, Australia

Received August 14, 2000

Mono- and dicopper(II) complexes of a series of potentially bridging hexaamine ligands have been prepared and characterized in the solid state by X-ray crystallography. The crystal structures of the following Cu^{II} complexes are reported: $[Cu(HL^3)](ClO_4)_3$, $C_{11}H_{31}Cl_3CuN_6O_{12}$, monoclinic, $P2_1/n$, $a = 8.294(2)$ Å, $b = 18.364(3)$ Å, $c = 15.674(3)$ Å, $\beta = 94.73(2)°$, $Z = 4$; $\{[Cu_2(L^4)(CO_3)]_2\}(ClO_4)_4 \cdot 4H_2O$, $C_{40}H_{100}Cl_4Cu_4N_{12}O_{26}$, triclinic, $P\bar{1}$, $a = 9.4888(8)$ Å, $b = 13.353(1)$ Å, $c = 15.329(1)$ Å, $\alpha = 111.250(7)°$, $\beta = 90.068(8)°$, $\gamma = 105.081(8)°$, $Z = 1$; $[Cu_2(L^5)(OH_2)_2](ClO_4)_4$, $C_{13}H_{36}Cl_4Cu_2N_6O_{18}$, monoclinic, $P2_1/c$, $a = 7.225(2)$ Å, $b = 8.5555(5)$ Å, $c = 23.134(8)$ Å, $\beta = 92.37(1)°$, $Z = 2$; $[Cu_2(L^6)(OH_2)_2](ClO_4)_4 \cdot 3H_2O$, $C_{14}H_{44}Cl_4Cu_2N_6O_{21}$, monoclinic, $P2_1/a$, $a = 15.204(5)$ Å, $b = 7.6810(7)$ Å, $c = 29.370(1)$ Å, $\beta = 100.42(2)°$, $Z = 4$. Solution spectroscopic properties of the bimetallic complexes indicate that significant conformational changes occur upon dissolution, and this has been probed with EPR spectroscopy and molecular mechanics calculations.

Introduction

Dicopper sites within metalloproteins feature prominently in bioinorganic chemistry, and synthetic model compounds have attracted much attention as a consequence.[1] Some relevant examples include the oxygen-binding protein hemocyanin[2] and the nitrite reductases.[3] Cooperative interactions between neighboring metal centers can play an important part in the structure and function of metalloproteins, and the relative orientation of the two metal coordination spheres is a crucial factor. In metalloproteins, the adjacent metal ions are typically held in position by the protein framework, but in model compounds, bridging ligands with separated metal coordinating sites are often employed. Various approaches have been adopted that employ rigid aromatic groups or flexible saturated bridges as scaffolds to which appropriate donor atoms are attached. It is also possible for monometallic complexes to self-assemble into a bimetallic structure via bridging ligands such as hydroxide, carbonate, or peroxide,[4] which obviates the need for a covalent link between the two chelating moieties.

A number of biological models have comprised bis-tridentate coordinating N-donor ligands to mimic histidine residues of the natural systems. The facially coordinating tridentate ligand 1,4,7-triazacyclotridecane has been extensively studied in this capacity,[5] where a bridge connects amines on different macrocycles. Additional donor groups have also been incorporated on the remaining amines of these ligands.[6] *cis*,*cis*-1,3,5-Triaminocyclohexane has also been employed in a similar way as a facially coordinating tridentate bridged by a rigid spacer.[7] Recently, a pyridyl-appended macrocyclic ether has also been reported, which forms a dicopper complex with O_2-binding activity.[8]

Recently we reported[9] the syntheses, crystal structures, and spectroscopic properties of the Cu^{II} complexes of the branched hexaamines L^1 and L^2. We found that the EDTA analogue L^1 binds as a pentadentate to give a trigonal bipyramidal monometallic Cu^{II} complex with one free aminoethyl "arm". By contrast, dimethylation of all primary amines to give the tertiary hexaamine L^2 generates a bridging ligand where two different Cu^{II} ions are bound in a meridional tridentate fashion by each

(1) (a) Kitajima, N.; Moro-oka, Y. *Chem. Rev.* **1994**, *94*, 737. (b) Karlin, K. D.; Kaderli, S.; Zuberbhhler, A. D. *Acc. Chem. Res.* **1997**, *30*, 139. (c) Tolman, W. B. *Acc. Chem. Res.* **1997**, *30*, 227.

(2) Kitajima, N.; Fujisawa, K.; Fujimoto, C.; Moro-oka, Y.; Hashimoto, S.; Kitagawa, T.; Toriumi, K.; Tatsumi, K.; Nakamura, A. *J. Am. Chem. Soc.* **1992**, *114*, 1277.

(3) Halfen, J. A.; Mahapatra, S.; Wilkinson, E. C.; Gengenbach, A. J.; Young, V. G. Jr.; Que, J., Jr.; Tolman, W. B. *J. Am. Chem. Soc.* **1996**, *118*, 763.

(4) (a) Halfen, J. A.; Mahapatra, S.; Wilkinson, E. C.; Kaderli, S.; Young, V. G., Jr.; Que, J., Jr.; Zuberbhhler, A. D.; Tolman, W. B. *Science* **1996**, *271*, 1397. (b) Sorrell, T. N.; Allen, W. E.; White, P. S. *Inorg. Chem.* **1995**, *34*, 952. (c) Darensbourg, D. J.; Holtcamp, M. W.; Khandelwal, B.; Reibenspies, J. H. *Inorg. Chem.* **1995**, *34*, 5390. (d) Kitajima, N.; Hikichi, S.; Tanaka, M.; Moro-oka, Y. *J. Am. Chem. Soc.*, **1993**, *115*, 5496.

(5) (a) Mahapatra, S.; Young, V. G., Jr., Kaderli, S.; Zuberbhhler, A. D.; Tolman, W. B. *Angew. Chem., Int. Ed. Engl.* **1997**, *36*, 130. (b) Haidar, R.; Ipek, M.; DasGupta, B.; Yousaf, M. J.; Zompa, L. J. *Inorg. Chem.*, **1997**, *36*, 3125. (c) Sessler, J. L.; Sibert, J. W.; Burrell, A. K.; Lynch, V. *Inorg. Chem.* **1993**, *32*, 4277. (d) Hanke, D.; Wieghardt, K.; Nuber, B.; Lu, R.; McMullan, R.; Kotzle, T.; Bau, R. *Inorg. Chem.*, **1993**, *32*, 4300.

(6) (a) Brudenell, S. J.; Spiccia, L.; Tiekink, E. R. T. *Inorg. Chem.* **1996**, *35*, 1975. (b) Brudenell, S. J.; Spiccia, L.; Bond, A. M.; Comba, P.; Hockless, D. C. R. *Inorg. Chem.* **1998**, *37*, 3705. (c) Blake, A. J.; Donlevy, T. M.; England, P. A.; Fallis, I. A.; Parsons, S.; Schröder, M. *J. Chem. Soc., Chem. Commun.* **1994**, 1981.

(7) Boxwell, C. J.; Bhalla, R.; Cronin, L.; Turner, S. S.; Walton, P. H. *J. Chem. Soc., Dalton Trans.* **1998**, 2449.

(8) Klein Gebbink, R. J. M.; Martens, C. F.; Kenis, P. J. A.; Jansen, R. J.; Nolting, H.-F.; Solé, V. A.; Feiters, M. C.; Karlin, K. D.; Nolte, R. J. M. *Inorg. Chem.* **1999**, *38*, 5755.

(9) Bernhardt, P. V.; Hayes, E. J. *J. Chem. Soc., Dalton Trans.* **1998**, 1037.

10.1021/ic000928s CCC: $20.00
Published on Web 02/03/2001

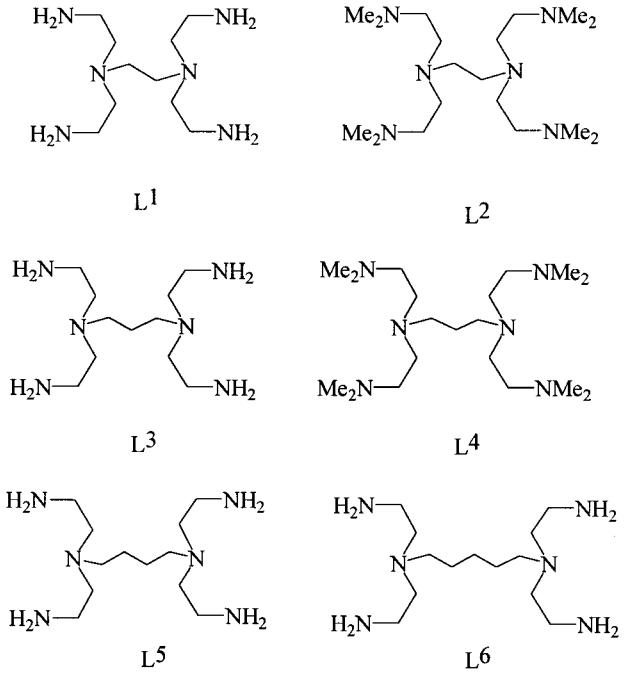

diethylenetriamine moiety. The steric effect of the N-methyl groups was the driving force for the preferred bis-tridentate coordination mode as opposed to a pentadentate- or hexadentate-coordinating mode.

Another way to achieve a bis-tridentate coordination mode is to increase the length of the bridge so that chelation by the diamine becomes unfavorable. For example, L^1 and L^3 should form 1:1 metal/ligand complexes comprising five- and six-membered chelate rings across the bridge. By contrast, the ligands L^5 and L^6 should favor 2:1 metal/ligand complexes, thus avoiding formation of inherently strained seven- and eight-membered chelate rings. We report the syntheses and characterization of the Cu^{II} complexes of the hexaamine L^3, its N-methylated derivative L,[4] and the extended ligands L^5 and L^6.

Experimental Section

Safety Note. Although we have experienced no problems with the compounds reported herein, perchlorate salts are potentially explosive and should only be handled in small quantities, never heated in the solid state or scraped from sintered glass frits.

Ligands. The hexaamines L^3·6HBr, L^5·6HBr, and L^6·6HBr were prepared by reaction of the appropriate linear diamine (1,3-propane-, 1,4-butane-, and 1,5-pentanediamine) with *N*-tosylaziridine in benzene at room temperature for 2 d followed by detosylation with HBr/AcOH, as described for the ethylene-bridged analogue,[10] then isolated as the hydrobromide salt after addition of an equal volume of EtOH/Et_2O (1:1) to the ice-cooled acidic mixture. The tertiary hexaamine L^4 was synthesized by refluxing L^3 in HCOOH/CH_2O as described previously[9] in the synthesis of L^2, and the free base was obtained by extraction of an alkaline solution of L^4 (pH ~12) with CH_2Cl_2. ^{13}C NMR: L^3·6HBr (D_2O) δ 21.5, 36.7, 52.4, 53.0 ppm; L^4 ($CDCl_3$) δ 24.4, 46.0, 52.7, 53.2, 57.8 ppm; L^5·6HBr (D_2O) δ 23.0, 36.5, 52.3, 55.6 ppm; L^6·6HBr (D_2O) δ 22.4 (accidental degeneracy), 33.7, 49.5, 53.6 ppm.

Complexes. $[Cu(HL^3)](ClO_4)_3$. A solution of $CuCl_2$·$2H_2O$ (0.70 g) and L^3·6HBr (3.0 g) in water (200 mL) was neutralized with dilute aqueous NaOH. The ensuing blue solution was charged on a Sephadex C-25 cation-exchange resin (Na^+ form). A major blue band ($[Cu(HL^3)]^{3+}$) eluted with 0.5 M $NaClO_4$, which precipitated on concentration to ca. 50 mL. The solid was collected by filtration and then washed with EtOH and Et_2O. $[Cu(HL^3)](ClO_4)_3$: yield, 1.05 g (42%) from first crop. Crystals suitable for X-ray work were obtained by slow evaporation of the filtrate. (Found: C, 21.5; H, 5.1; N, 13.5. Calcd for $C_{11}H_{31}Cl_3CuN_6O_{12}$: C, 21.7; H, 5.1; N, 13.8)

The complexes $\{[Cu_2(L^4)(CO_3)]_2\}(ClO_4)_4$·$H_2O$, $[Cu_2(L^5)(OH_2)_2](ClO_4)_4$, and $[Cu_2(L^6)(OH_2)_2](ClO_4)_4$ were all prepared by reaction of the free ligand, or ligand hydrobromide with 2 equiv of $Cu(NO_3)_2$·$3H_2O$ in aqueous solution (adjusted to pH 7 with NaOH solution) followed by cation exchange column chromatography as described above. Crystals of $\{[Cu_2(L^4)(CO_3)]_2\}(ClO_4)_4$·$H_2O$ and $[Cu_2(L^5)(OH_2)_2](ClO_4)_4$ were grown from concentrated aqueous solutions of the complex, whereas crystals of $[Cu_2(L^6)(OH_2)_2](ClO_4)_4$ were obtained by vapor diffusion of CH_2Cl_2 into an EtOH solution of the complex. $\{[Cu_2(L^4)(CO_3)]_2\}(ClO_4)_4$·$6H_2O$.$2NaClO_4$. Found: C, 26.0; H, 5.4; N, 9.0. Calcd for $C_{40}H_{104}Cl_6Cu_4N_{12}NaO_{36}$: C, 26.1; H, 5.7; N, 9.1. $[Cu_2(L^5)(OH_2)_2](ClO_4)_4$. Found: C, 17.5; H, 4.4; N, 10.2. Calcd for $C_{12}H_{36}Cl_4Cu_2N_6O_{18}$: C, 17.6; H, 4.4; N, 10.2. $[Cu_2(L^6)](ClO_4)_4$. Found: C, 20.7; H, 4.7; N, 11.0. Calcd for $C_{13}H_{34}Cl_4Cu_2N_6O_{16}$: C, 19.4; H, 4.8; N, 10.5.

Physical Methods. Solution UV−vis spectra were measured on a Perkin-Elmer Lambda 12 spectrophotometer. Infrared spectra were measured with a Perkin-Elmer 1600 series spectrometer with all compounds being dispersed as KBr disks. X-Band (ca. 9.3 GHz) electron paramagnetic resonance spectra were measured on a Bruker ER200 D spectrometer as frozen 1 mM solutions (1:2 DMF/water, 77 K). Spin Hamiltonian parameters were obtained by spectral simulation using EPR50F[11] for monometallic complexes and DISSIM[12] for bimetallic complexes. For the bimetallic spectra, in addition to the expected strong $\Delta M_s = \pm 1$ transitions, broad and weak "half-field" ($\Delta M_s = \pm 2$) transitions were observed at ca. 1500 G, but these were of little diagnostic value because of their poor resolution and intensity.

Molecular Mechanics. Molecular mechanics calculations were performed with MOMEC[13] using a published force field.[14] The N-methylated bimetallic complexes $[Cu_2(L^2)(OH_2)_2]^{4+}$ and $[Cu_2(L^4)(OH_2)_2]^{4+}$ were modeled as five-coordinate, square pyramidal complexes with an additional aqua ligand in the apical site of each metal center. The remaining complexes $[Cu_2(L^5)(OH_2)_2]^{4+}$ and $[Cu_2(L^6)(OH_2)_2]^{4+}$ were modeled with tetragonally elongated octahedral coordination geometries, with trans pairs of weakly bound aqua ligands coordinated in the sites perpendicular to each CuN_3O plane. This choice was based on the crystal structure geometries of the species, where steric effects of the N-methyl groups block the approach of a second axial ligand. In the primary amine analogues ($[Cu_2(L^5)(OH_2)_2]^{4+}$ and $[Cu_2(L^6)(OH_2)_2]^{4+}$) no such steric effects are present and tetragonally elongated six-coordinate geometries ensue.

In each case, the conformational lability of the five-membered chelate rings was ignored, and the eclipsed conformation found in the crystal structure geometries was assumed to be present. This assumption does not affect the relative orientations of the two metal centers. For the complexes $[Cu_2(L^2)(OH_2)_2]^{4+}$ ($n = 3$), $[Cu_2(L^4)(OH_2)_2]^{4+}$ ($n = 4$), $[Cu_2(L^5)(OH_2)_2]^{4+}$ ($n = 5$), and $[Cu_2(L^6)(OH_2)_2]^{4+}$ ($n = 6$) all 3^n conformations were considered on the basis of the three local torsional angle minima (trans, gauche(+), and gauche(−)) for each N−C or C−C bond along the flexible methylene bridge connecting the two metal centers. Not every conformer was unique or nondegenerate, and some conformations were rejected on the basis of excessive steric repulsion. Minimized strain energies from the entire conformational analysis of each complex are presented as Supporting Information.

Crystallography. Cell constants were determined by a least-squares fit to the setting parameters of 25 independent reflections measured on an Enraf-Nonius CAD4 four-circle diffractometer employing graphite monochromated Mo Kα radiation (0.710 73 Å) and operating in the $\omega-2\theta$ scan mode. Data reduction, Lorentz, polarization, and empirical

(10) Wagnon, B. K.; Jackels, S. C. *Inorg. Chem.* **1989**, *28*, 1923.
(11) Martinelli, R. A.; Hanson, G. R.; Thompson, J. S.; Holmquist, B.; Pilbrow, J. R.; Auld, D. S.; Vallee, B. L. *Biochemistry* **1989**, *28*, 2251.
(12) Pilbrow, J. R.; Smith, T. D. *Coord. Chem. Rev.* **1974**, *13*, 173.
(13) Comba, P.; Hambley, T. W.; Lauer, G.; Okon, P. *MOMEC, A Molecular Mechanics Program for Coordination Compounds* (adapted to HyperChem); Heidelberg, Germany, 1995.
(14) Bernhardt, P. V.; Comba, P. *Inorg. Chem.*, **1992**, *31*, 2638.

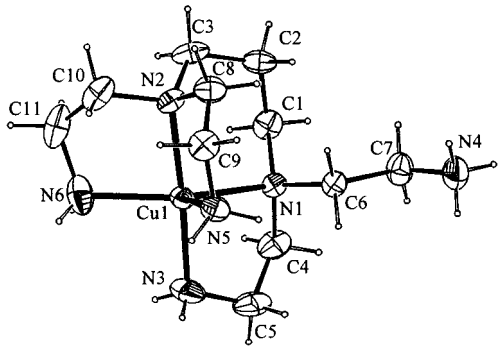

Figure 1. View of the $[Cu(HL^3)]^{3+}$ cation (30% probability ellipsoids). Selected bond lengths (Å) and angles (deg) are the following: Cu1−N3 1.985(4); Cu1−N2 2.029(4); Cu1−N6 2.079(5); Cu1−N5 2.162(4); Cu1−N1 2.164(4); N3−Cu1−N2 176.3(2); N3−Cu1−N6 91.9(2); N2−Cu1−N6 84.9(2); N3−Cu1−N5 99.4(2); N2−Cu1−N5 83.8(2); N6−Cu1−N5 117.7(2); N3−Cu1−N1 84.9(2); N2−Cu1−N1 96.2(2); N6−Cu1−N1 138.3(2); N5−Cu1−N1 103.8(2).

absorption corrections (ψ scans) were performed with the XTAL[15] package except for the $[Cu_2(L^5)(OH_2)_2](ClO_4)_4$ and $[Cu_2(L^6)(OH_2)_2](ClO_4)_4 \cdot 3H_2O$ data sets, which were not corrected for absorption (no suitable ψ-scan reflections could be located).

Structure Solutions. Structures were solved by heavy atom methods with SHELXS-86[16] and refined by full-matrix least-squares analysis with SHELXL-97.[17] All non-H atoms were refined with anisotropic thermal parameters except disordered perchlorate O atoms and C atoms included in one disordered chelate ring in the structure of $\{[Cu_2(L^4)(CO_3)]_2\}(ClO_4)_4 \cdot 4H_2O$. Hydrogen atoms were included at estimated positions and constrained using a riding model. Selected bond lengths and angles appear in the captions of Figures 1−4 drawn with PLATON.[18]

Results and Discussion

Syntheses of the trimethylene- and tetramethylene-bridged hexaamines L^3 and L^5 have been reported previously,[19] using *N*-benzenesulfonyl aziridine as the aminoethylating agent. The procedure followed here uses *N*-tosylaziridine (derived from *N*-tosyl-2-chloroethylamine), avoiding the hazardous aziridine as a precursor to *N*-benzenesulfonyl aziridine.[20] All Cu^{II} complexes formed immediately upon neutralizing aqueous solutions of metal and ligand, and purification was achieved using cation exchange chromatography.

Solid-State Structures. The crystal structure of $[Cu(HL^3)](ClO_4)_3$ reveals a monometallic complex exhibiting a distorted trigonal bipyramidal coordination geometry where one of the aminoethyl arms (namely, N4) is protonated (Figure 1). A measure of the distortion from trigonal bipyramidal geometry is given by the parameter ϕ, which is defined as the difference between the two largest N−Cu−N angles divided by 60. In this case $\phi = 0.63$; $\phi = 1$ for an ideal trigonal bipyramid, while $\phi = 0$ for a square pyramid. The axial bonds to N2 and N3 are somewhat shorter than those made with the three equatorial N donors. The structure is similar to that of the analogue $[Cu(HL^1)](ClO_4)_3$ ($\phi = 0.46$)[9] but is evidently closer to trigonal bipyramidal geometry. The reason for this difference in the degree of distortion can be appreciated by considering the adjacent five-membered chelate rings in $[Cu(HL^1)]^{3+}$ that span the N2−Cu1−N3 axis and reduce the trans angle to 167°, compared with the more accommodating alternating six- and five-membered chelate rings in $[Cu(HL^3)]^{3+}$, which allow the trans N2−Cu1−N3 angle to extend to 176°.

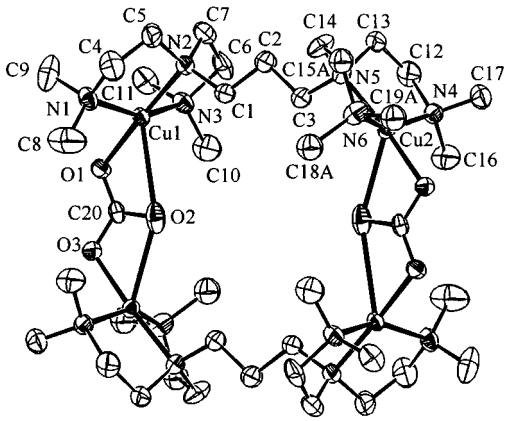

Figure 2. View of the $\{[Cu_2(L^4)(CO_3)]_2\}^{2+}$ cation (30% probability ellipsoids). H atoms have been omitted for clarity. Selected bond lengths (Å) and angles (deg) are the following: Cu1−O1 1.922(5); Cu1−N2 2.009(6); Cu1−N1 2.036(6); Cu1−N3 2.047(6); Cu1−O2 2.718(7); Cu2−O3$^{\#}$ 1.936(5); Cu2−N5 2.014(5); Cu2−N6 2.029(6); Cu2−N4 2.051(6); O2−Cu2$^{\#}$ 2.529(7); O1−Cu1−N2 177.0(2); O1−Cu1−N1 93.6(2); N2−Cu1−N1 86.5(2); O1−Cu1−N3 95.4(2); N2−Cu1−N3 85.8(2); N1−Cu1−N3 153.2(3); O1−Cu1−O2 53.8(2); N2−Cu1−O2 123.2(2); N1−Cu1−O2 104.9(2); N3−Cu1−O2 100.8(2); O3$^{\#}$−Cu2−N5 175.5(2); O3$^{\#}$−Cu2−N6 94.5(2); N5−Cu2−N6 86.0(3); O3$^{\#}$−Cu2−N4 95.4(2); N5−Cu2−N4 86.1(2); N6−Cu2−N4 151.4(3); Cu2$^{\#}$−O2−Cu1 151.9(2). The symbol # represents the symmetry transformation $-x, -y, -z + 1$.

The X-ray crystal structure of $\{[Cu_2(L^4)(CO_3)]_2\}(ClO_4)_4 \cdot 4H_2O$ revealed a novel sixteen-membered metallomacrocyclic structure incorporating two bridging carbonato ligands, derived from absorption of atmospheric CO_2 (Figure 2). The carbonato ligands are approximately symmetrically disposed between the two metals (Cu1−O1, Cu2$^{\#}$−O3 ≈ 1.9 Å; Cu1−O2, Cu2$^{\#}$−O2 ≈ 2.6 Å), but the Cu−O bond lengths within each four-membered chelate ring to each metal are clearly quite different. There exist a number of polymetallic carbonato Cu^{II} complexes that exhibit a similar bridging mode.[21] However, one unusual feature of the present structure is that the carbonato ligand is asymmetrically coordinated to each Cu atom, in contrast to the majority of Cu^{II} complexes of this class. The asymmetric coordination of the carbonato ligand has its origins in the Jahn−Teller effect operative on the d^9 electronic ground state of each metal center. In this case, the ensuing axial elongation coincides with the Cu−O2 coordinate bonds. By contrast, in other bridged carbonato complexes, the direction of axial distortion is usually perpendicular to the Cu−O_2CO plane, and the two Cu−O bonds do not differ greatly in general. The Cu−Cu separations within the centrosymmetric Cu_4 rectangular array are 5.091(1) Å (across the bridging carbonate), 7.912(1) Å (across the C-3 bridge), 9.313(2) Å (diagonal Cu1···Cu1$^{\#}$), and 9.502(2) Å

(15) Hall, S. R., Flack, H. D., Stewart, J. M., Eds. *The XTAL3.2 User's Manual*; Universities of Western Australia, Geneva, and Maryland, 1992.
(16) Sheldrick, G. M. *Acta Crystallogr., Sect. A* **1990**, *46*, 467.
(17) Sheldrick, G. M. *SHELXL-97: Program for Crystal Structure Determination*; University of Göttingen: Göttingen, Germany, 1997.
(18) Spek, A. L. *Acta Crystallogr., Sect. A* **1990**, *46*, C34.
(19) Hata, K.; Doh, M.-K.; Kashiwabara, K.; Fujita, J. *Bull. Chem. Soc. Jpn.* **1981**, *54*, 190.
(20) Moser, P.; Schwarzenbach, G. *Helv. Chim. Acta* **1952**, *35*, 2359.
(21) (a) Churchill, M. R.; Davies, G.; El-Sayed, M. A.; Hutchinson, J. P. *Inorg. Chem.* **1982**, *21*, 1002. (b) Churchill, M. R.; Davies, G.; El-Sayed, M. A.; El-Shazly, M. F.; Hutchinson, J. P.; Rupich, M. W.; Watkins, K. O. *Inorg. Chem.* **1979**, *18*, 2296. (c) Davis, A. R.; Einstein, F. W. B. *Inorg. Chem.* **1980**, *19*, 1203. (d) Sletten, J.; Hope, H.; Julve, M.; Kahn, O.; Verdaguer, M.; Dvorkin, A. A. *Inorg. Chem.* **1988**, *27*, 542. (e) Kitajima, N.; Fujisawa, K.; Koda, T.; Hikichi, S.; Moro-oka, Y. *J. Chem. Soc., Chem. Commun.* **1990**, 1357. (f) Kitajima, N.; Koda, T.; Hashimoto, S.; Kitagawa, T.; Moro-oka, Y. *J. Am. Chem. Soc.* **1991**, *113*, 5664.

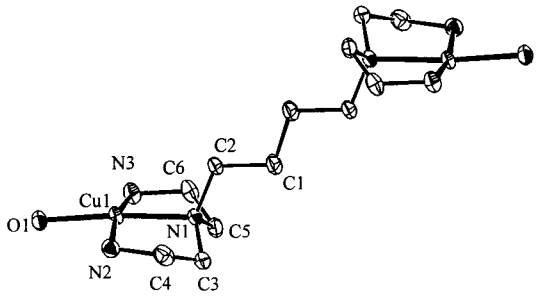

Figure 3. View of the $\{[Cu_2(L^5)(OH_2)_2]^{4+}$ cation (30% probability ellipsoids). H atoms have been omitted for clarity. Selected bond lengths (Å) and angles (deg) are the following: Cu1−N2 1.922(3); Cu1−N3 1.923(3); Cu1−O1 1.984(3); Cu1−N1 2.021(3); N2−Cu1−N3 168.34(15); N2−Cu1−O1 92.84(13); N3−Cu1−O1 93.97(13); N2−Cu1−N1 87.64(13); N3−Cu1−N1 84.67(14); O1−Cu1−N1 174.35(12).

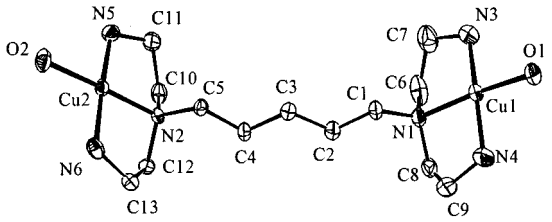

Figure 4. View of the $\{[Cu_2(L^6)(OH_2)_2]^{4+}$ cation (30% probability ellipsoids). H atoms have been omitted for clarity. Selected bond lengths (Å) and angles (deg) are the following: Cu1−N3 1.965(8); Cu1−O1 1.977(6); Cu1−N4 1.980(9); Cu1−N1 2.034(7); Cu2−N6 1.980(7); Cu2−O2 1.993(6); Cu2−N5 2.000(7); Cu2−N2 2.016(6); N3−Cu1−O1 96.6(3); N3−Cu1−N4 167.3(5); O1−Cu1−N4 90.1(4); N3−Cu1−N1 87.3(3); O1−Cu1−N1 175.8(3); N4−Cu1−N1 85.8(4); N6−Cu2−O2 95.3(3); N6−Cu2−N5 168.6(3); O2−Cu2−N5 92.4(3); N6−Cu2−N2 86.0(3); O2−Cu2−N2 174.6(3); N5−Cu2−N2 85.5(3).

(diagonal Cu2···Cu2#). The observation that N-methylation of the primary amines of this class leads to 2:1 metal/ligand complexes was first demonstrated for the mono- and bimetallic complexes of the ligands L^1 and L^2, respectively.[9] In this case, a similar result is obtained where the steric bulk of the dimethylamino arms disfavors a 1:1 metal/ligand complex, which would require the simultaneous coordination of five or six tertiary amines to the one metal center.

The solid-state IR spectrum of $\{[Cu_2(L^4)(CO_3)]_2\}(ClO_4)_4 \cdot 4H_2O$ exhibited a number of prominent peaks that were absent in all other Cu^{II} complexes in this series, specifically carbonato ligand vibrations at 1445, 1418, and 839 cm^{-1}. The IR spectrum of the powder isolated from the chromatographic purification of $\{[Cu_2(L^4)(CO_3)]_2\}(ClO_4)_4 \cdot 4H_2O$ was identical to that obtained from the crystals used for X-ray analysis. Recrystallization of $\{[Cu_2(L^4)(CO_3)]_2\}(ClO_4)_4 \cdot 4H_2O$ from MeCN/diethyl ether afforded crystals that were identical to those grown from aqueous solution.

The crystal structure of $[Cu_2(L^5)(OH_2)_2](ClO_4)_4$ reveals a bimetallic complex (Figure 3) where centrosymmetrically related metal centers are coordinated to separate diethylenetriamine groups in addition to an equatorial aqua ligand and weakly bound axial ClO_4^- anions. The all-trans conformation of the tetramethylene bridge is similar to that seen in the structure of $\{[Cu_2(L^4)(CO_3)]_2\}(ClO_4)_4 \cdot 4H_2O$, except that the even number of C atoms leads to an anti disposition of the two metal ions, separated by 9.685(3) Å. Unlike its di- and trimethylene-bridged relatives (L^1 and L^3), the tetramethylene-bridged hexaamine L^5 evidently does not form a 1:1 metal/ligand complex, but instead a bridged bimetallic complex is formed in preference to a strained seven-membered chelate ring incorporating the 1,4-butanediamine fragment.

The crystal structure of $[Cu_2(L^6)(OH_2)_2](ClO_4)_4$ again shows two CuN_3O units bridged by a pentamethylene chain (Figure 4). Weak axial bonds to the two independent Cu^{II} centers are made by ClO_4^- anions. The Cu−Cu separation is 10.759(3) Å, and the disposition of the two metal centers is syn as a result of the odd-numbered (five) carbon atom bridge. Again, the conformation of the bridge is all trans. No significant intermolecular contacts are present other than H-bonding involving water molecules and ClO_4^- anions.

Solution Structures. The solution spectroscopic properties of the monometallic $[Cu(HL^3)]^{3+}$ ion are unique among all other complexes reported in this work. The visible electronic maxima for this complex ($\epsilon_{\sim 850nm} \approx 190$ M^{-1} cm^{-1} (shoulder), $\epsilon_{732nm} = 210$ M^{-1} cm^{-1}, and $\epsilon_{\sim 650nm} \approx 170$ M^{-1} cm^{-1} (shoulder)) are very similar to those reported for the distorted trigonal bipyramidal relative $[Cu(HL^1)]^{3+}$, and an assignment of these transitions has been given elsewhere.[9] The frozen solution EPR spectra of $[Cu(HL^3)]^{3+}$ and $[Cu(HL^1)]^{3+}$ are also indistinguishable and again consistent with distorted trigonal bipyramidal monometallic Cu^{II} complexes; $g_x = 2.264$ ($A_x = 131$ G), $g_y = 2.140$ ($A_y = 25$ G), $g_z = 2.025$ ($A_z = 25$ G). It is clear that the distorted trigonal bipyramidal structures identified in the solid state for both $[Cu(HL^1)]^{3+}$ and $[Cu(HL^3)]^{3+}$ are retained in solution.

Of particular interest to this study was the solution behavior of the bimetallic complexes. The lability and structural diversity of Cu^{II} complexes do not, in general, allow one to assume that the local coordination geometry observed in the solid state is maintained in solution, unlike complexes of typically inert metal ions. Variations in both coordination number and stoichiometry of the Cu^{II}/ligand assembly can result upon dissolution, so spectroscopic measurements are a vital accompaniment to any structural study. Moreover, in this case, the flexible methylene bridges may adopt many different conformations, which will influence the relative orientations of the two coordinated metal ions.

Electronic spectroscopy is very useful in defining the local coordination environment of each complex. Although all complexes are blue, the energy of the single visible maximum is sensitive to the types of N donors present. The visible electronic maxima of the Cu^{II} complexes of the tertiary amines L^4 ($\epsilon_{698nm} = 240$ M^{-1} cm^{-1} per Cu^{II}) and $[Cu_2(L^2)(OH_2)_2]^{4+}$ ($\epsilon_{704nm} = 210$ M^{-1} cm^{-1} per Cu^{II})[9] are essentially the same. This is consistent with dissociation of the tetrametallic complex $\{[Cu_2(L^4)(CO_3)]_2\}(ClO_4)_4$ in solution to generate a bimetallic complex of the form $[Cu_2(L^4)(OH_2)_2]^{4+}$, and this was confirmed by EPR spectroscopy (see below). The UV−vis spectra of $[Cu_2(L^5)(OH_2)_2]^{4+}$ ($\epsilon_{620nm} = 104$ M^{-1} cm^{-1} per Cu^{II}) and $[Cu_2(L^6)(OH_2)_2]^{4+}$ ($\epsilon_{620nm} = 88$ M^{-1} cm^{-1} per Cu^{II}) are also consistent with pseudo-square-planar $Cu^{II}N_3O$ chromophores. The higher energy visible maxima found in the spectra of $[Cu_2(L^5)(OH_2)_2]^{4+}$ and $[Cu_2(L^6)(OH_2)_2]^{4+}$ reflect the shorter Cu−N bond lengths observed in the crystal structures of the primary amine complexes compared with their more sterically crowded tertiary amine analogues.

Dipole−dipole coupling of the two d^9 ions (nuclear spin $1^1/_2$) within a dicopper(II) complex typically results in an EPR spectrum quite unlike those of monometallic analogues. Simulation of the EPR spectrum provides information such as Cu−Cu distance and the relative orientation (parallel, orthogonal, etc.) of the two CuN_3O planes within the bimetallic complex.[12] The frozen solution EPR spectra of $[Cu_2(L^4)(OH_2)_2]^{4+}$, $[Cu_2(L^5)(OH_2)_2]^{4+}$, and $[Cu_2(L^6)(OH_2)_2]^{4+}$ were measured and simulated (Figure 5). The three dicopper(II) compounds exhibit

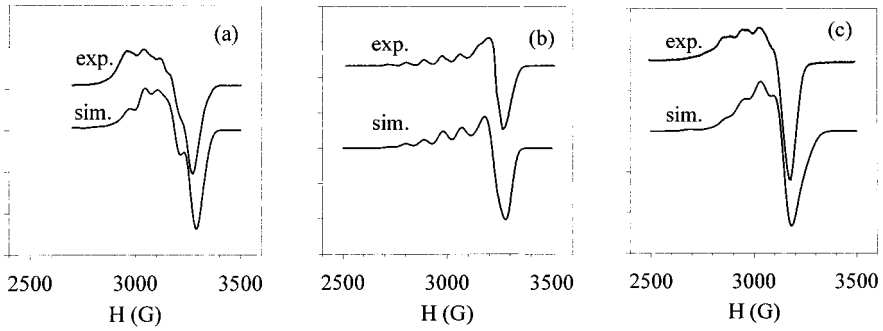

Figure 5. Experimental and simulated frozen solution EPR spectra of (a) $[Cu_2(L^4)(OH_2)_2]^{4+}$, (b) $[Cu_2(L^5)(OH_2)_2]^{4+}$, and (c) $[Cu_2(L^6)(OH_2)_2]^{4+}$ (10^{-3} mol dm^{-3} solutions of complex in 1:2 DMF/H_2O, spectrometer frequency of 9.3 GHz).

Table 1. Crystal Data

	$[Cu(HL^3)][(ClO_4)_3$	$\{[Cu_2(L^4)(CO_3)]_2\}(ClO_4)_4\cdot 4H_2O$	$[Cu_2(L^5)(OH_2)_2](ClO_4)_4$	$[Cu_2(L^6)(OH_2)_2](ClO_4)_4\cdot 3H_2O$
formula	$C_{11}H_{31}Cl_3CuN_6O_{12}$	$C_{40}H_{100}Cl_4Cu_4N_{12}O_{26}$	$C_{12}H_{36}Cl_4Cu_2N_6O_{18}$	$C_{13}H_{44}Cl_4Cu_2N_6O_{21}$
fw	609.3	1561.3	821.35	889.42
space group	$P2_1/n$ (No. 14[a])	$P\bar{1}$ (No. 2)	$P2_1/c$ (No. 14)	$P2_1/a$ (No. 14[a])
a, Å	8.294(2)	9.4888(8)	7.225(2)	15.204(5)
b, Å	18.364(3)	13.353(1)	8.5555(5)	7.6810(7)
c, Å	15.674(3)	15.329(1)	23.134(8)	29.370(1)
α, deg		111.250(7)		
β, deg	94.73(2)	90.068(8)	92.37(1)	100.42(2)
γ, deg		105.081(8)		
V, Å^3	2379.2(8)	1750.5(2)	1428.8(6)	3373(2)
Z	4	1	2	4
temp, °C	23	23	23	23
λ, Å	0.710 73	0.710 73	0.710 73	0.710 73
μ, cm^{-1}	13.23	14.30	19.51	16.66
ρ_{calc}, g cm^{-3}	1.701	1.481	1.909	1.751
$R(F_o)^b$	0.0521	0.0684	0.0440	0.0669
wR2(F_o^2)[c]	0.1287	0.1880	0.1201	0.1877

[a] Variant of $P2_1/c$. [b] $R(F_o) = \sum||F_o| - |F_c||/\sum|F_o|$. [c] $wR2(F_o^2) = (\sum w(F_o^2 - F_c^2)/\sum wF_o^2)^{1/2}$.

Table 2. Solid-State and Solution Structures of Each Dinuclear Copper(II) Complex

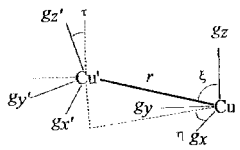

	crystal structure					solution structure[a]				
	conformation[b]	r_{Cu-Cu} (Å)	ξ (deg)	τ (deg)	η (deg)	conformation[b]	r_{Cu-Cu} (Å)	ξ (deg)	τ (deg)	η (deg)
$[Cu_2(L^2)(OH_2)_2]^{4+}$	t,t,t	7.2	74	0	0	t,t,t	7.1	74	0	0
$[Cu_2(L^4)(OH_2)_2]^{4+}$	t,t,t,t	7.9	45	90	0	+,t,t,+	6.0	67	70	45
$[Cu_2(L^5)(OH_2)_2]^{4+}$	t,t,t,t,t	9.7	63	0	0	+,+,+,+,+	7.5	30	5	90
$[Cu_2(L^6)(OH_2)_2]^{4+}$	t,t,t,t,t,t	10.7	50	70	0	+,t,+,+,t,+	6.6	5	8	90

[a] Estimated uncertainties in the simulation geometric parameters are ±0.2 Å in the distances and ±5° in the angles. [b] t = trans; + = gauche(+), − = gauche(−).

similar spin Hamiltonian parameters, consistent with their comparable coordination environments: $[Cu_2(L^4)(OH_2)_2]^{4+}$ $g_{||} = 2.315$ ($A_{||} = 107$ G), $g_\perp = 2.075$ ($A_\perp = 24$ G); $[Cu_2(L^5)(OH_2)_2]^{4+}$ $g_{||} = 2.285$ ($A_{||} = 92$ G), $g_\perp = 2.050$ ($A_\perp = 16$ G); $[Cu_2(L^6)(OH_2)_2]^{4+}$ $g_{||} = 2.275$ ($A_{||} = 95$ G), $g_\perp = 2.115$ ($A_\perp = 31$ G). On the other hand, the structural parameters (r_{Cu-Cu}, ξ, τ, and η) are quite different because the length of the alkyl chain connecting the two metal centers is different in each case. Moreover, we found that the solution conformations of the new dicopper(II) complexes reported herein are totally different from those defined by their respective crystal structure analyses (Table 2). The corresponding published data[9] for $[Cu_2L^2(OH_2)_2]^{4+}$ has been included for comparison. All remaining EPR simulation parameters are included as Supporting Information. To illustrate the structural sensitivity of this technique, we have also calculated the EPR spectrum of each complex in its crystal structure geometry by keeping the spin Hamiltonian parameters the same as those found in the actual simulation (Supporting Information). In each case, the spectrum calculated from the solid-state structure is clearly different from that measured experimentally.

Dissociation of the carbonato-bridged metallomacrocycle identified in the crystal structure of $\{[Cu_2(L^4)(CO_3)]_2\}(ClO_4)_4\cdot 4H_2O$ is evident from a simulation of the bimetallic spectrum. Furthermore, the EPR spectrum of $[Cu_2(L^4)(OH_2)_2]^{4+}$ was unaffected by saturation of the solution with CO_2 prior to freezing (data not shown). This reinforces the UV−vis spectroscopic results, which indicated that the carbonato complex is not a major species in solution and only forms in the solid state because of its lower solubility.

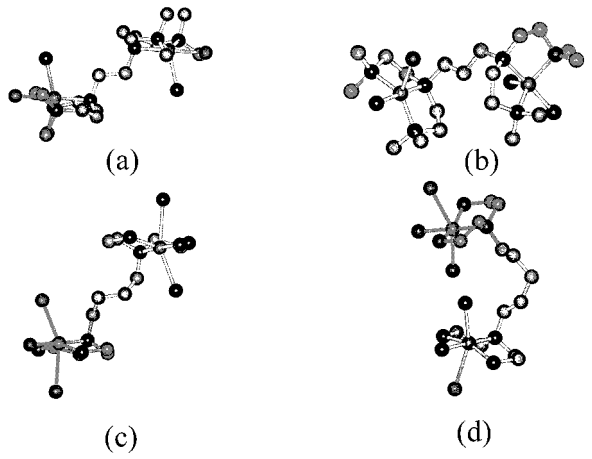

Figure 6. Solution structures (modeled with molecular mechanics calculations) of (a) $[Cu_2(L^2)(OH_2)_2]^{2+}$, (b) $[Cu_2(L^4)(OH_2)_2]^{2+}$, (c) $[Cu_2(L^5)(OH_2)_2]^{2+}$, and (d) $[Cu_2(L^6)(OH_2)_2]^{2+}$. H atoms are omitted for clarity.

Conformational Analysis. There are a number of parameters to be refined in a typical EPR simulation, and obtaining a unique fit is often difficult. The spin Hamiltonian (*g* and *A*) parameters obtained from the simulation should be comparable across a homologous series of complexes such as those found here. On the other hand, the structural parameters (r_{Cu-Cu}, ξ, τ, and η) must be able to be accommodated by physically reasonable conformations of the bridging ligand. In principle all possible conformers of each ligand can be examined and refined using molecular mechanics calculations. However, the number of conformers becomes intractable even for the smallest bridging ligand (L^2) unless some assumptions are made. In this case, we ignore the conformational flexibility of the five-membered chelate rings of each diethylenetriamine unit and retain the conformation observed in each crystal structure. It is clear that the various λ and δ combinations of the four five-membered chelate rings in each dicopper(II) complex have no effect on the Cu−Cu separation or the orientation of the two metal coordination spheres. This leaves the torsional angles defined by the C−N and C−C single bonds in the bridge as the only significant conformational degrees of freedom. There are three energy minima (trans, gauche(+), and gauche(−)) for a C−C or C−N single bond. For each additional single bond in the bridge, the number of possible conformers is multiplied by 3. For $[Cu_2(L^2)(OH_2)_2]^{4+}$ this results in 27 (3^3) stable rotamers, whereas for $[Cu_2(L^6)(OH_2)_2]^{4+}$ the system comprises 729 (3^6) possible stable rotamers, many of which are degenerate because of symmetry. The problem is further simplified by the omission of all conformations where adjacent gauche torsional angles have opposite sense, i.e., gauche(+) and gauche(−). Such gauche (+)/(−) pairs generate conformers where the terminal groups in the five-atom chain clash. The conformation analysis for all dicopper(II) complexes reported here has been deposited as Supporting Information. Given that molecular mechanics calculations take no account of solvation or other intermolecular interactions, it is crucial that solution spectroscopic measurements accompany these calculations in an effort to test the predictions of this relatively simple model.

1. $[Cu_2(L^2)(OH_2)_2]^{4+}$. This complex has been reported previously,[9] and the crystal structure geometry was found to be essentially the same as that found in solution from an EPR spectral analysis (Table 2). Molecular mechanics analysis revealed that this all-trans (t,t,t) conformer (Figure 6a) has the lowest strain energy but is only 1.6 kJ mol^{-1} lower than the corresponding trans,trans,gauche(+) (t,t,+) conformer.

2. $[Cu_2(L^4)(OH_2)_2]^{4+}$. As mentioned above, the tetrametallic complex identified crystallographically (Figure 2) dissociates into discrete dicopper(II) complexes in solution. The all-trans (t,t,t,t) conformer (identified in the crystal structure of the tetracopper(II) analogue) possesses the lowest strain energy, but a number of other conformers have strain energies within 1 kJ mol^{-1} of this, including the conformer identified in solution (Figure 6b), namely, the (+,t,t,+) conformer. Twisting of the formerly all-trans trimethylene bridge brings the two Cu^{II} ions 1.9 Å closer than in the crystal structure conformation.

3. $[Cu_2(L^5)(OH_2)_2]^{4+}$. The (+,+,+,+,+) conformation of the tetramethylene bridge was identified in solution (Figure 6c), which is completely different from that found in the crystal structure analysis (t,t,t,t,t). Interestingly, coiling of the tetramethylene bridge in solution draws the two Cu^{II} centers 2.2 Å closer together while keeping the two CuN_3O planes parallel. The conformer with the lowest strain energy (*t,t,+,t,t)* was ca. 30 kJ mol^{-1} lower in energy than the observed (+,+,+,+,+) conformer.

4. $[Cu_2(L^6)(OH_2)_2]^{4+}$. The solution conformation (+,t,+,+,t,+) shown in Figure 6d possesses a strain energy some 14 kJ mol^{-1} higher than a cluster of low-energy conformers, including the crystallographically observed (t,t,t,t,t,t) conformer (Figure 4). The two near-parallel CuN_3O planes were found to be almost coaxial, and the Cu−Cu separation was more than 4 Å smaller than that seen in the crystal structure conformation.

Molecular mechanics calculations take no account of intermolecular interactions such as solvation and ion pairing; i.e., they are "gas-phase" calculations. Therefore, the discrepancies between the observed solution structures and those predicted on the basis of the lowest strain energy highlight the limitations and potential pitfalls of molecular mechanics calculations in isolation. The driving force for the marked contraction of the intramolecular Cu−Cu separation going from the solid state to solution in $[Cu_2(L^4)(OH_2)_2]^{4+}$, $[Cu_2(L^5)(OH_2)_2]^{4+}$, and $[Cu_2(L^6)(OH_2)_2]^{4+}$ is uncertain, although solvation forces are most probably responsible. Presumably, the hydrophobic polymethylene chain twists so as to avoid interactions with water molecules in solution, thus drawing the two metal centers closer together. It is apparent that this is not taken into account within the molecular mechanics model, and higher level theoretical studies need to be undertaken to clarify this point.

Conclusions

This study has revealed that conformationally flexible complexes such as the polymethylene-bridged bimetallic systems reported may adopt unusual and unexpected conformations in solution that are distinctly different from those in the solid state. Molecular mechanics calculations were helpful in defining physically reasonable solution conformations, although the calculated strain energies were of little use in a predictive sense. We have shown how a preference for bimetallic, bis-tridentate coordination of the hexaamine ligands in this series may be promoted either by extension of the bridging polymethylene chain (disfavoring chelation) or by N-methylation of the terminal amines (steric effects). In terms of complex design to favor a particular orientation of the two coordination sites, it is clear that rigidity in the bridging group must be built in. This may be possible through the fusion of phenyl or cyclohexyl rings onto the bridge, and this warrants further investigation.

Acknowledgment. Technical assistance of Mr. David Hunter with the EPR measurements is gratefully acknowledged. We

are also grateful for financial assistance from the Australian Research Council and the University of Queensland.

Supporting Information Available: Crystallographic data, in CIF format, EPR simulation parameters, calculated EPR spectra based on solid-state and solution structures, and a full molecular mechanics conformational analysis. This material is available free of charge via the Internet at http://pubs.acs.org.

IC000928S